武漢科技大学
WUHAN UNIVERSITY OF SCIENCE AND TECHNOLOGY

The 9th International Symposium on Refractories

Comparative study on microstructures and properties of Al_2O_3-$MgAl_2O_4$-C ceramic filter and Al_2O_3-C ceramic filter

Speaker: **Jinwen Song**
Supervisor: **Prof. Wen YAN**
Wuhan University of Science and Technology

2024 CHENGDU·CHINA

CONTENT

厚德博學 崇實去浮

1

PART ONE

武汉科技大学
Wuhan University of Science and Technology

Research background

Research background

武漢科技大學
WUHAN UNIVERSITY OF SCIENCE AND TECHNOLOGY

Under the background of "Made in China 2025" policy, the demand for ultra-clean steel in major equipment manufacturing and major engineering construction in China is increasing day by day.

Non-metallic inclusion in steel is one of the important factors that affects steel properties and safety applications. Therefore, how to reduce the non-metallic inclusions and improve the quality of steel is a problem that needs to be solved at present.

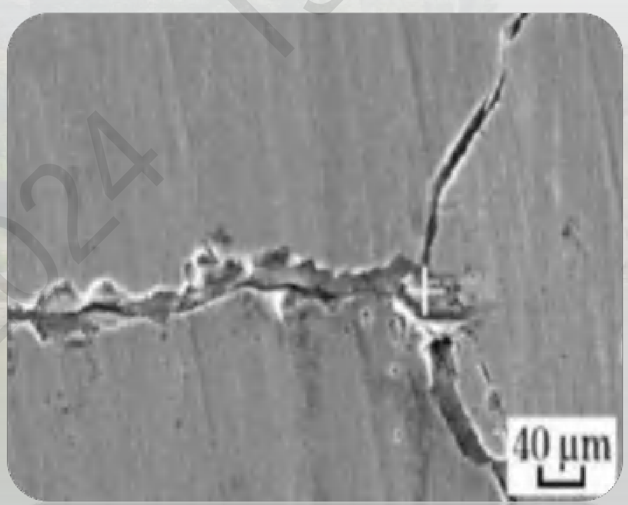

Research background

WUHAN UNIVERSITY OF SCIENCE AND TECHNOLOGY

The porous ceramic filter has a three-dimensional network structure, a porosity of up to 70-90%, and a large surface area, mainly used in the final procedure of steel casting, which is one of the effective ways to adsorb and filter the non-metallic inclusions in molten steel.

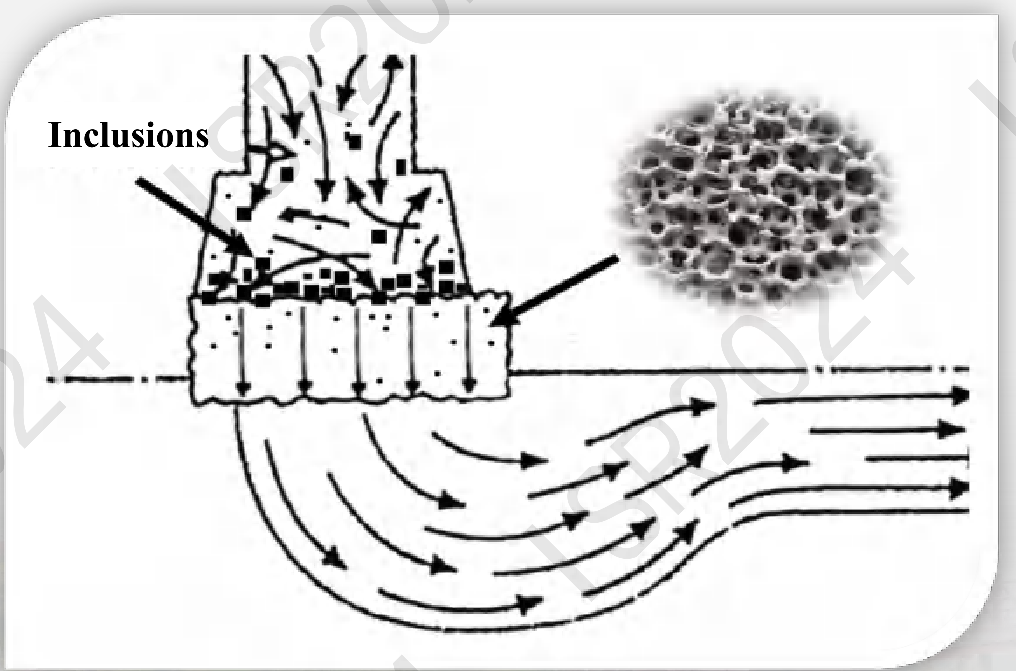

CaO filter → Easy hydration

SiC filter → Low filtration efficiency

Zr_2O filter → Poor volume stability

Al_2O_3 filter → Poor thermal shock resistance

Al_2O_3-C filter → ☑ **Excellent filtration performance, thermal shock resistance and creep resistance**

Research background

武漢科技大學
WUHAN UNIVERSITY OF SCIENCE AND TECHNOLOGY

The inherent limitations of the Al_2O_3-C materials

① In the aspect of sintering of strut, **carbon is an inert phase in sintering theory**, and **it is difficult to form a strong neck bond between carbon and Al_2O_3**, limiting the further enhancement of thermal shock resistance.

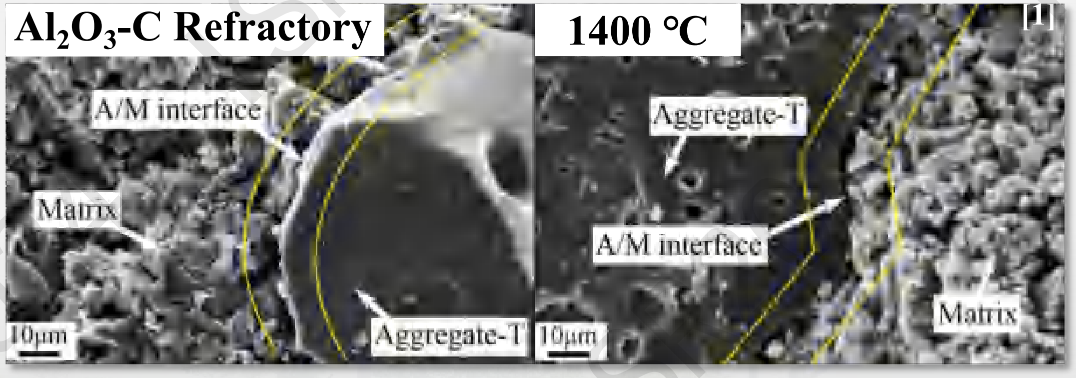

Limit the further improvement of thermal shock resistance and strength!

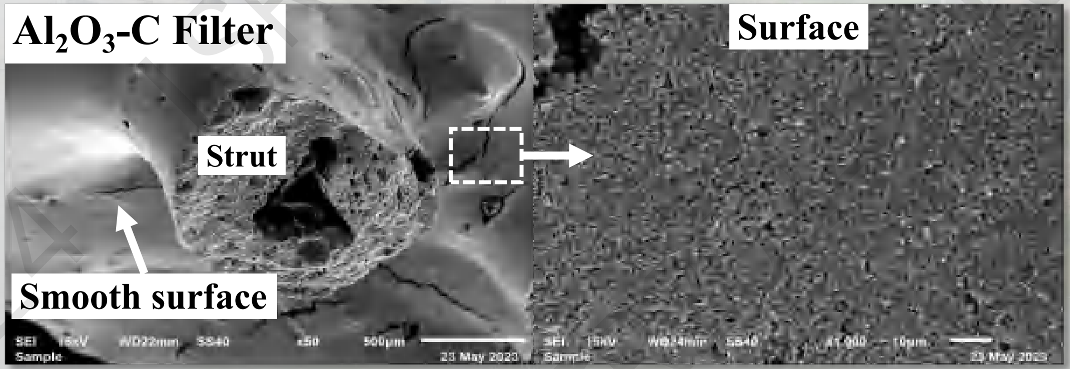

② In the other aspect of adsorption of inclusions, the **smooth surface of dense Al_2O_3 leads to a small contact area and contact angle with molten steel**, thereby limiting the further improvement of inclusion adsorption and purification efficiency.

Limit the further improvement of inclusion adsorption and purification efficiency!

厚德博學 崇實去浮

[1] Z. Chen, W. Yan, S. Schaffoner, Y.W. Li, M. Nath, C.Y. Zhu, Enhanced mechanical properties of lightweight Al2O3-C refractories reinforced by combined one-dimensional ceramic phases, Int. J. Appl. Ceram. Tec. 19 (3) (2022) 1613–1625.

Research background

武漢科技大學
WUHAN UNIVERSITY OF SCIENCE AND TECHNOLOGY

Firstly, pore is an important component of the microstructure.

MgO ceramic filter

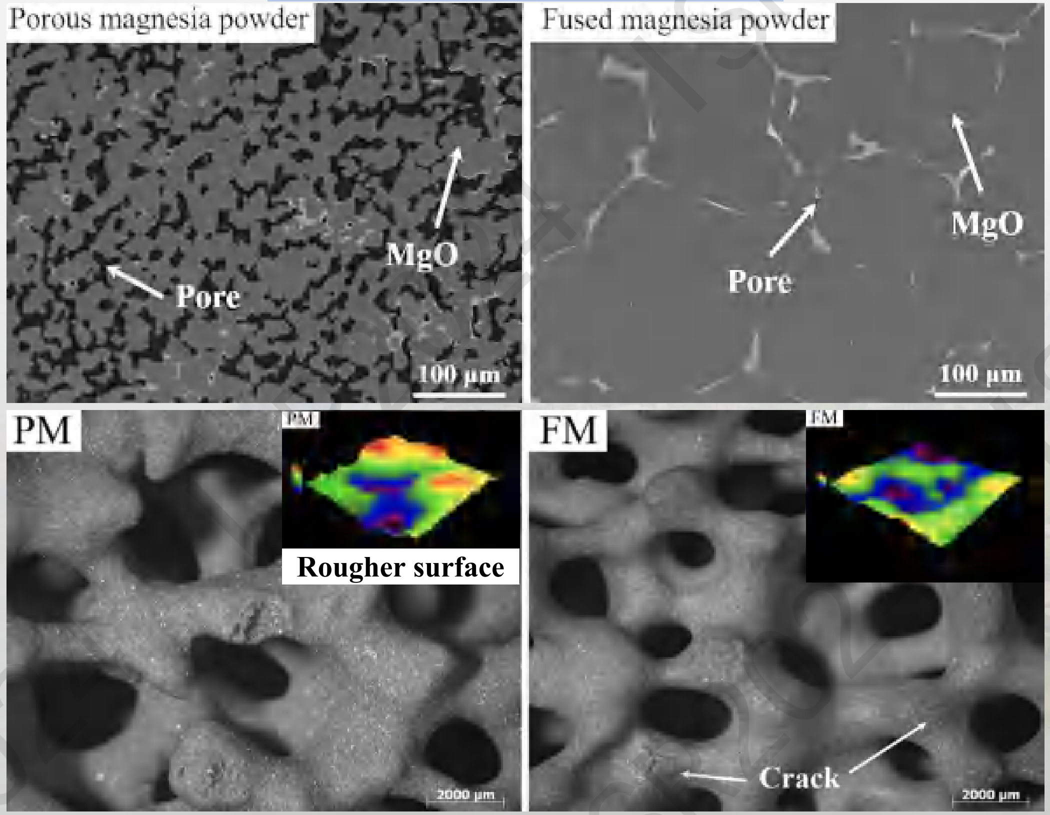

Physical properties	PM	FM
Bulk density of filter (g/cm³)	0.91 ± 0.01	0.88 ± 0.03
Apparent porosity of filter (%)	74.0 ± 0.01	74.1 ± 0.03
CCS (MPa)	**1.71 ± 0.11**	1.46 ± 0.09
CCS_{TS} (MPa)	**1.32 ± 0.08**	1.08 ± 0.05
Retention rate of CCS (%)	**77.2**	74.0

UP

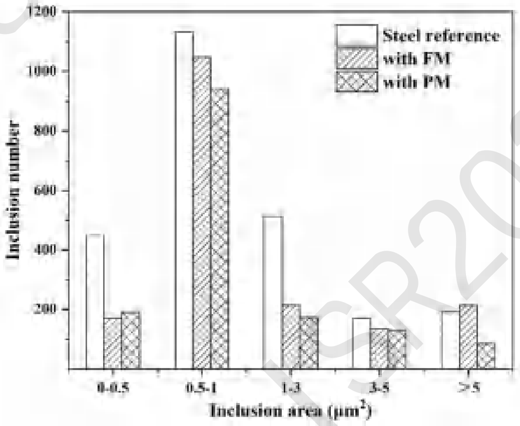

Chemical compositions of the steel samples

	C (wt%)	Al (wt%)	T.O (ppm)
Steel reference	0.100	0.250	37.5
with FM	0.054	0.084	33.1
with PM	0.054	0.072	29.4

厚德博學 崇實去浮

[2] Y. Liu, W. Yan, Z. Chen, J.F. Chen, Y. Liu, G.Q. Li, Preparation of high performance MgO ceramic filter and its interaction with molten steel: Effect of porous MgO powder, J. Eur. Ceram. Soc. 43 (8) (2023) 3794–3803.

Research background

武漢科技大學
WUHAN UNIVERSITY OF SCIENCE AND TECHNOLOGY

Secondly, $MgAl_2O_4$ is a crucial phase for enhancing the thermal shock resistance of MgO-Al_2O_3 system materials.

MgO-$MgAl_2O_4$ ceramic filter

MgO

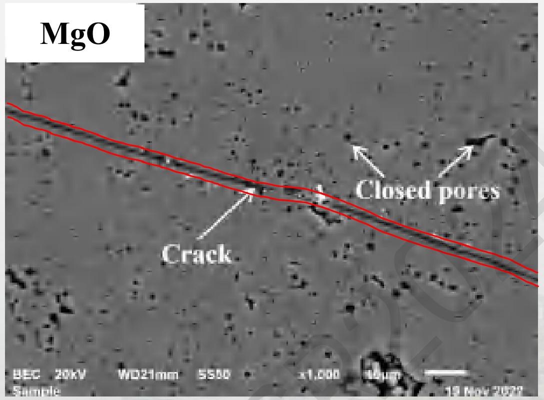

MgO-$MgAl_2O_4$

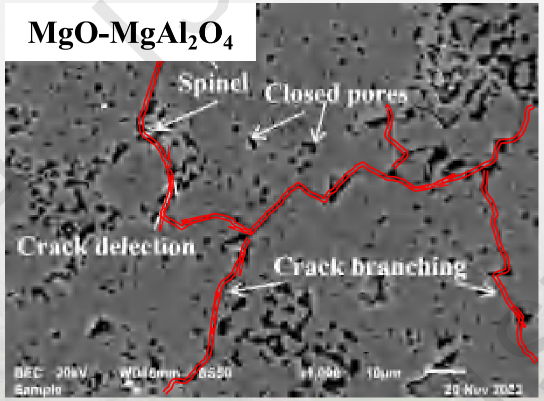

Physical properties	MA0	MA5	MA10	MA15	MA20
Bulk density of strut (g/cm^3)	2.52	2.77	2.85	2.87	2.96
Apparent porosity of strut (%)	28.8	22.3	20.4	20.1	17.0
CCS (MPa)	**1.68**	**2.04**	**1.78**	**1.84**	**2.35**
CCS_{TS} (MPa)	**1.29**	**1.93**	**1.56**	**1.62**	**1.91**
Retention rate of CCS (%)	**76.7**	**94.6**	**87.6**	**88.0**	**81.3**

Al_2O_3-$MgAl_2O_4$ ceramic filter

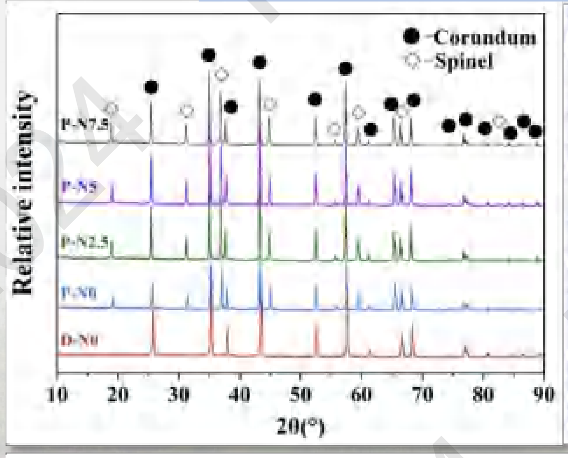

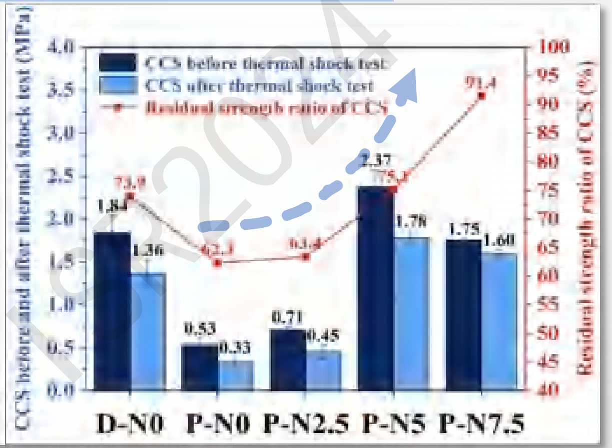

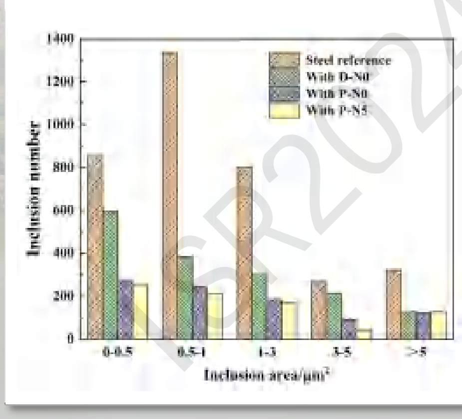

Chemical compositions of the steel samples

	Al (wt%)	T.O (ppm)
Steel reference	0.46	40.2
with D-N0	0.25	21.0
with P-N0	0.18	16.6
with P-N5	**0.18**	**12.7**

厚德博學 崇實去浮

[3] Y. Liu, W. Yan, Y. Liu, Q. Wang, G.Q. Li, N. Li, Effect of α-Al2O3 content on microstructures, mechanical properties and purification efficiency on molten steel of MgO-based filters, J. Eur. Ceram. Soc. 43 (14) (2023) 6516–6526.
[4] Z. Chen, W. Yan, G.Q. Li, S.S. Hong, N. Li, Enhanced mechanical properties of novel Al2O3-based ceramic filter by using microporous corundum-spinel and nano-Al2O3 powders, J. Eur. Ceram. Soc. 44 (2) (2024) 1070–1080.
[5] Z. Chen, W. Yan, Y. Liu, G.Q. Li, S.S. Hong, N. Li, Purification performance on molten steel of novel Al2O3-based ceramic filter prepared from microporous powder and nano-Al2O3 powder, J. Iron Steel Res. Int. 31 (2024) 1535-1546.

Research background

WUHAN UNIVERSITY OF SCIENCE AND TECHNOLOGY

Thirdly, the synergistic effect of the porous structure and β-SiC whiskers is an effective approach to enhancing the mechanical properties of Al_2O_3-C materials.

Physical properties	Aggregate T	Aggregate M
Bulk density (g/cm³)	3.54±0.02	2.82±0.02
True density (g/cm³)	3.904±0.003	3.967±0.003
Apparent porosity (%)	6.2±1	25.7±1
Closed porosity (%)	3.1±1	3.2±1
Total porosity (%)	**9.3±1**	**28.9±1**

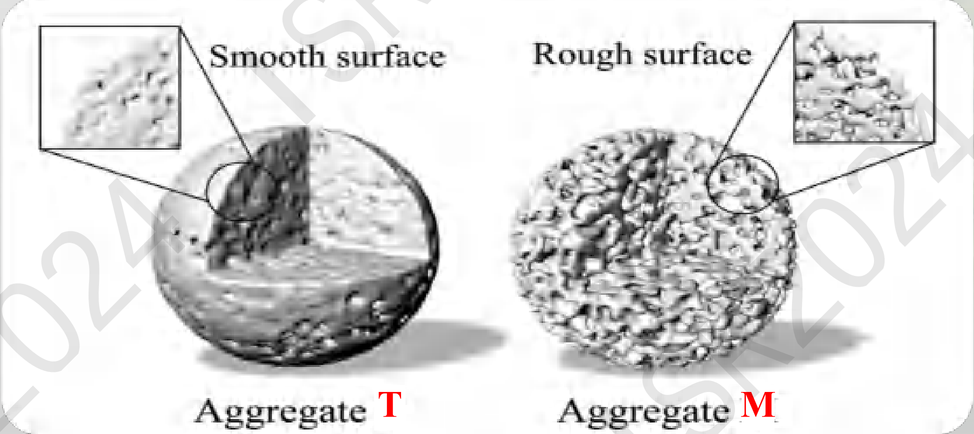

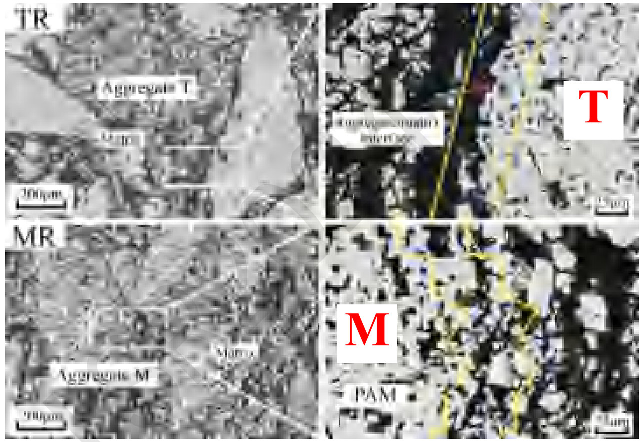

Physical properties of refractories

	TRS	MRS
Bulk density (g/cm³)	2.87	2.66
Apparent porosity (%)	17.4	23.3
CMOR (MPa)	**18.2**	**23.7**

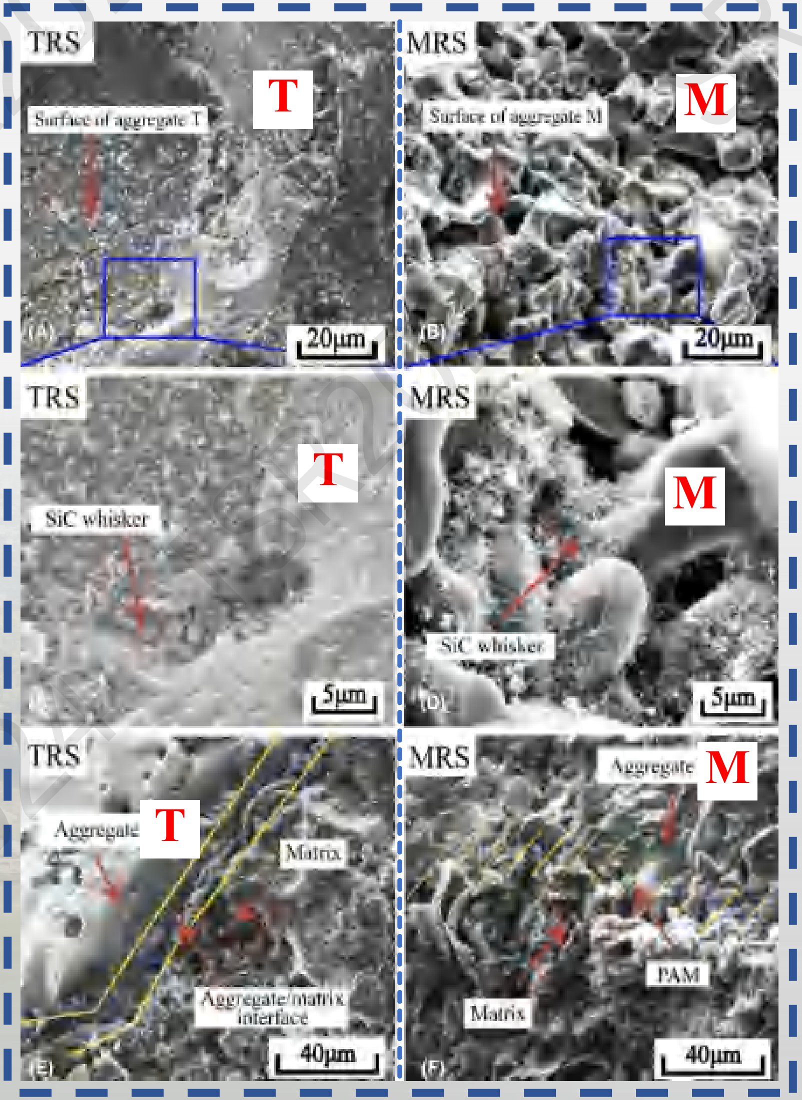

[6] Z. Chen, W. Yan, S. Schaffoner, Y.J. Dai, Q. Wang, G.Q. Li, A novel approach to lightweight alumina-carbon refractories for flow control of molten steel, J. Am. Ceram. Soc. 103 (8) (2020) 4713–4724.
[7] Z. Chen, W. Yan, S. Schaffoner, Y.W. Li, M. Nath, C.Y. Zhu, Enhanced mechanical properties of lightweight Al2O3-C refractories reinforced by combined one-dimensional ceramic phases, Int. J. Appl. Ceram. Tec. 19 (3) (2022) 1613–1625.

Research background

① Porous structure

② $MgAl_2O_4$ phase

③ β-SiC whisker-reinforced

Al_2O_3-$MgAl_2O_4$-C Ceramic Filter

Enhanced thermal shock resistance

Higher purification efficiency

We propose the utilization of **porous Al_2O_3-$MgAl_2O_4$ micropowder**, high-reactive **nano-carbon black**, and **Si powder** to prepare the Al_2O_3-$MgAl_2O_4$-C filter. This approach aims to **enhance thermal shock resistance through the synergistic toughening effects of β-SiC whiskers and the $MgAl_2O_4$ phase**, while also **improving the purification efficiency for molten steel by increasing the surface roughness of the filter's porous struts**.

2

— PART TWO —

武汉科技大学
Wuhan University of Science and Technology

Experiment procedures

Experiment procedures

Composition of the slurries (wt%)

		AM	A
Solids	**Porous Al_2O_3-$MgAl_2O_4$ micropowder**	**80**	0
	α-Al_2O_3 micropowder AMA-10	0	80
	Si	6	6
	Carbores®P	6	6
	Nano-Carbon Black N220	8	8
Additives[a]	Carboxymethyl cellulose C804619	0.36	0.36
	Lignosulfonate C804808	1.5	1.5
	Polycarboxylate WSM-M	0.3	0.3
	Glydol N1055	0.3	0.3
	Contraspum K1012	0.1	0.1

a Related to 100wt% solids

Porous Al_2O_3-$MgAl_2O_4$ raw material

Bulk density: 2.53 g/cm³; Apparent Porosity: 33.6%

Prepared by **in situ decomposition pore-forming technique**[8-10].

The filters prepared with **porous Al_2O_3-$MgAl_2O_4$ micropowder** were named **AM**.

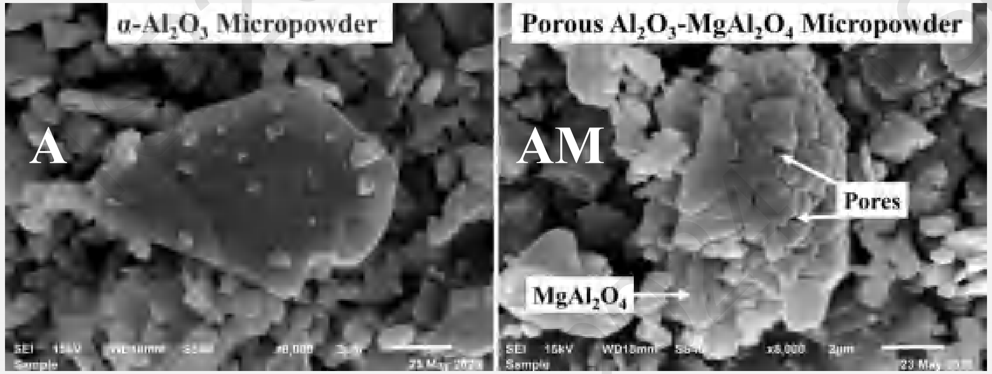

Chemical composition of the raw materials (wt%)

	α-Al_2O_3 micropowder	Porous Al_2O_3-$MgAl_2O_4$ micropowder
Al_2O_3	99.31	90.01
MgO	0.01	8.60
SiO_2	0.25	0.33
CaO	0.08	0.15
Fe_2O_3	0.07	0.41
K_2O	0.01	0.02
Na_2O	0.05	0.15
TiO_2	0.01	0.04
IL	-	0.12

[8] Z. Chen, W. Yan, S. Schafföner, J.N. Zhi, N. Li, Vacuum impregnation treatment of microporous Al2O3-MgAl2O4 refractory raw materials with sub-micron pores and high strength, J. Eur. Ceram. Soc. 42 (12) (2022) 5145–5152.
[9] W. Yan, G.Y. Wu, S.B. Ma, S. Schafföner, Y.J. Dai, Z. Chen, Energy efficient lightweight periclase-magnesium alumina spinel castables containing porous aggregates for the working lining of steel ladles, J. Eur. Ceram. Soc. 48 (12) (2018) 4276–4282.
[10] W. Yan, J.F. Chen, N. Li, W.D. Qiu, Y.W. Wei, B.Q. Han, Preparation and characterization of porous MgO-Al2O3 refractory aggregates using an in-situ decomposition pore-forming technique, Ceram. Int. 41 (1) (2015) 515–520

Experiment procedures

Immersion experiment

Al-killed steel (Wuhan Iron & Steel Co., China) was used in the immersion tests with a melting point of approximately 1540 °C and a composition of **C 0.063 wt%, Al 0.46 wt%, Si 0.017 wt%, S 0.017 wt%, Mn 0.051 wt%.** 200g of steel was used for each immersion experiment.

The immersion experiment was performed in a high-frequency induction furnace in a rotating magnetic field. The high purity **argon** with a purity of 99.99 % was slowly introduced with a flow rate of 0.5 L/min. When the temperature reached **1600 °C**, the filter was slowly immersed in the molten steel for **20 min** before the filter was separated from the molten steel and furnace-cooled.

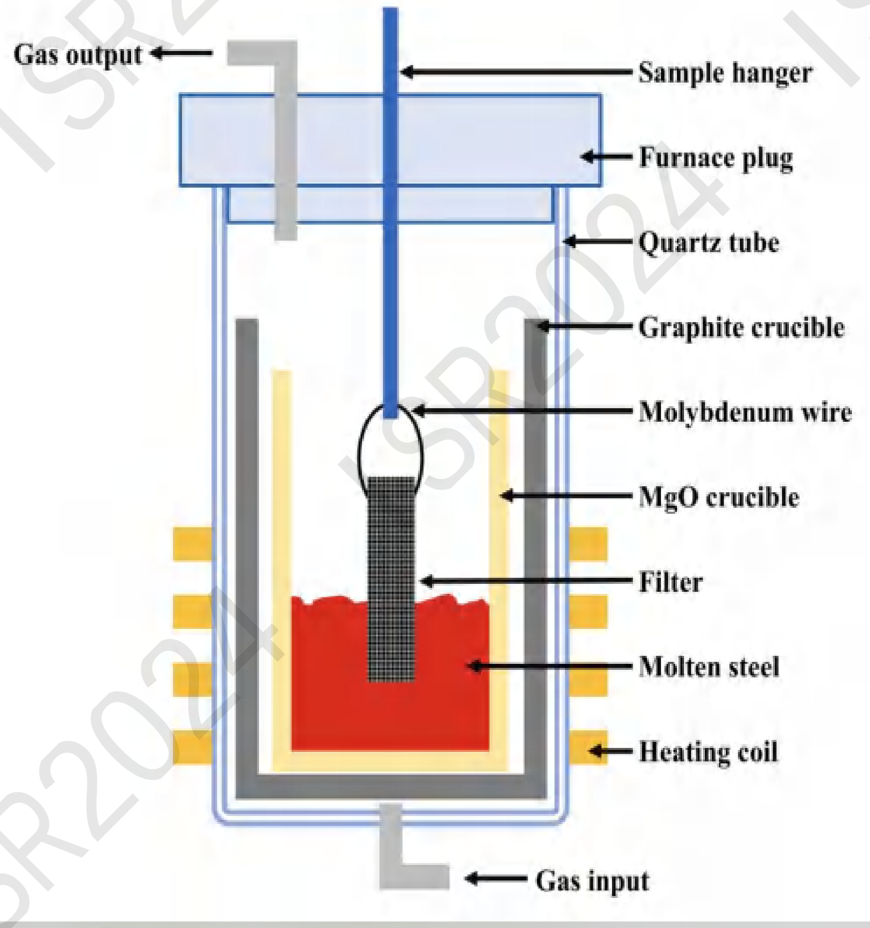

Schematic of set-up for the immersion experiment

3

—— PART THREE —

武汉科技大学
Wuhan University of Science and Technology

Results and discussion

Results and discussion

Phase compositions (XRD results)

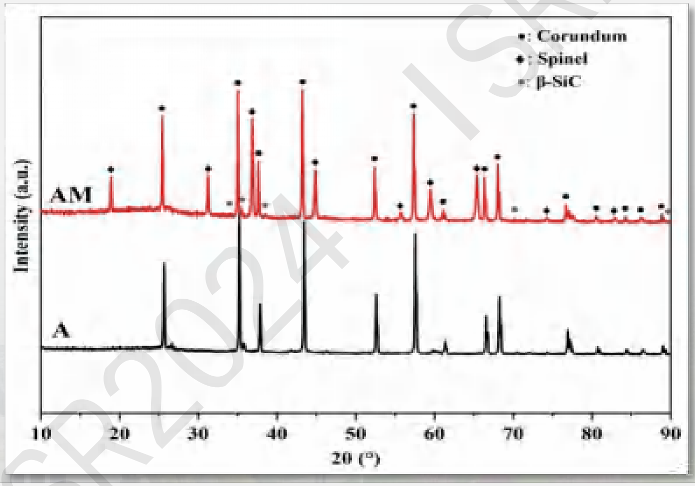

Relative contents of phase in the specimens (wt%)

	Corundum	Spinel	β-SiC
AM	58	33	9
A	97	-	3

Morphologies of the filters

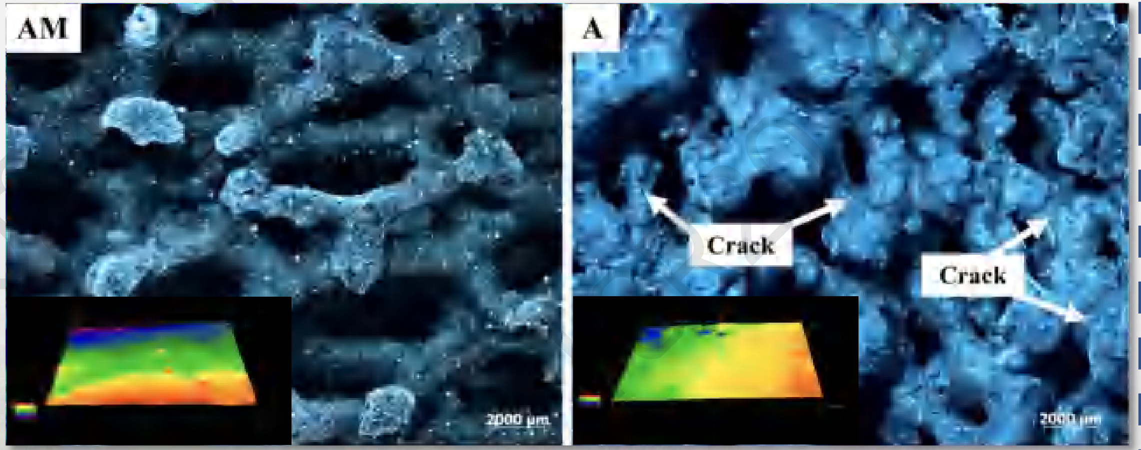

Surface roughness parameters of the substrates AM and A

	R_q/μm	R_a/μm	R_z/μm	R_{SA}
AM	0.799	0.626	3.055	1.072
A	0.393	0.303	1.520	1.021

Results and discussion

Microstructures of the filters

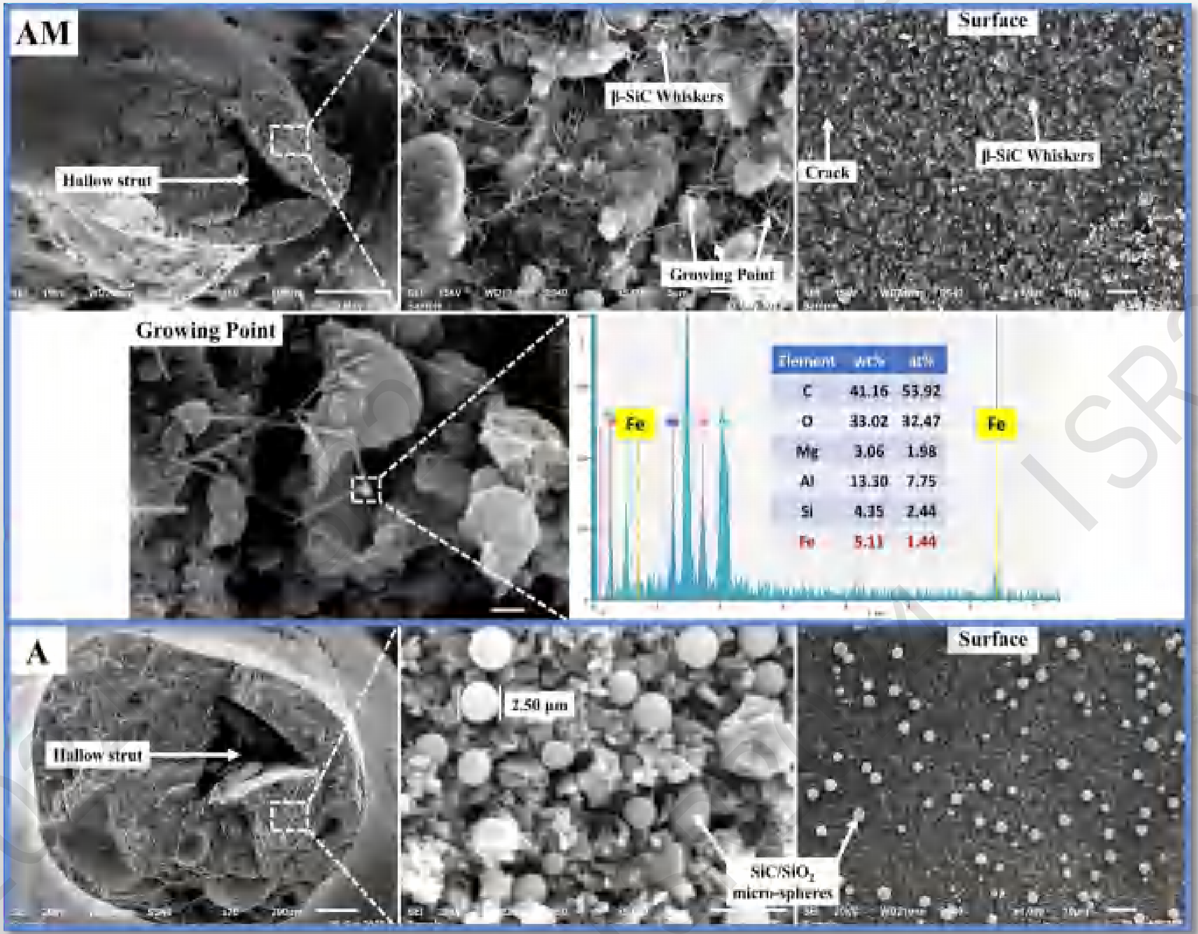

Physical properties of the filters

	AM	A
Bulk density of filter (g/cm³)	0.76±0.05	0.89±0.08
Porosity of filter (%)	57.30±2.81	43.31±5.09
CCS (MPa)	0.45±0.10	0.62±0.03
CCS_{TS} (MPa)	0.41±0.12	0.36±0.13
Retention rate of CCS (%)	91.11	58.06

Filter AM exhibited a **lower bulk density** and a **higher porosity**. The cold compressive strength of filter A was 37.78% higher than that of filter AM. However, **after three thermal shock tests, filter AM demonstrated a higher cold compressive strength** than that of filter A. Specifically, **filter AM retained 91.11%** of its original strength, while filter A only retained 58.06%.

Results and discussion

Interaction between the filters and molten steel

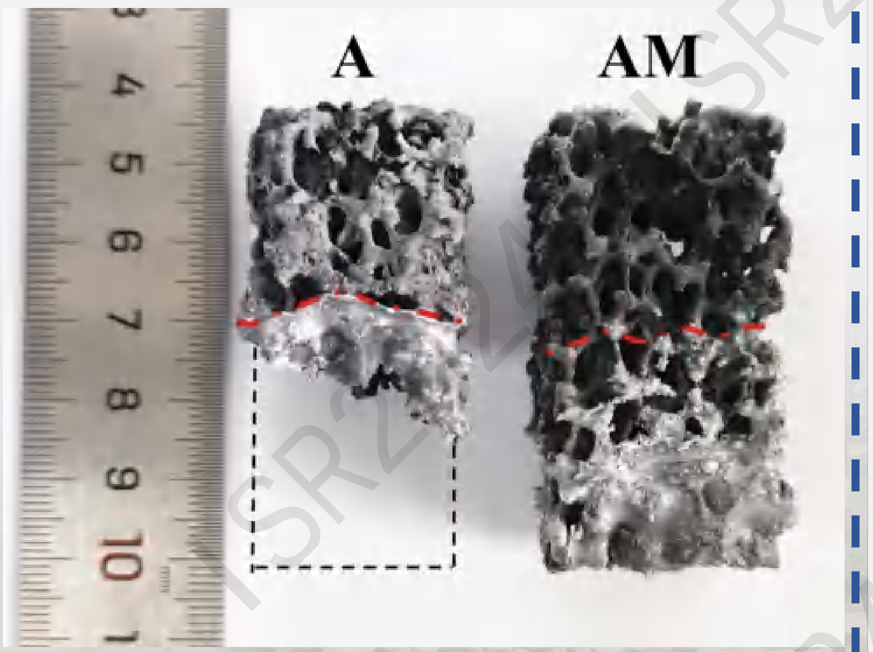

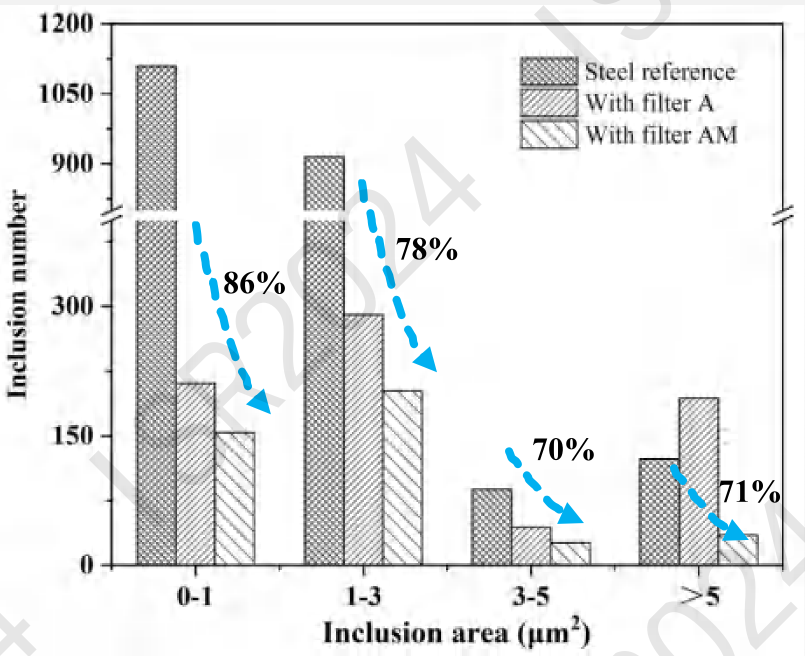

Inclusions

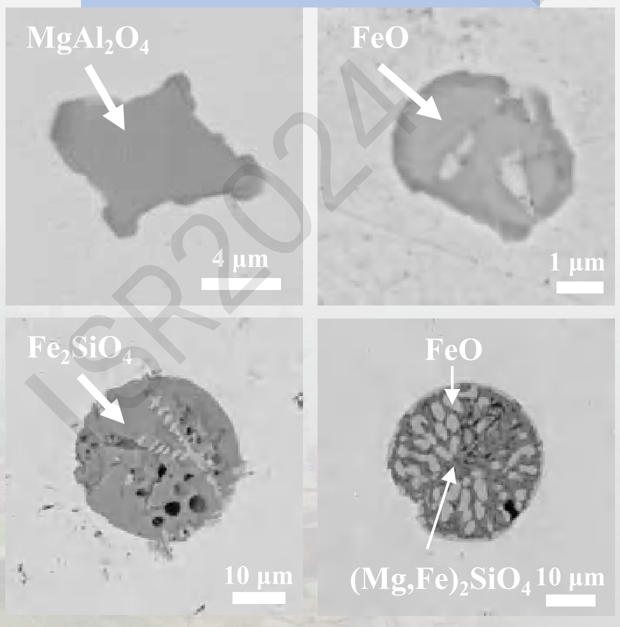

After immersion in the molten steel, **filter AM retained integrity**. Conversely, **filter A experienced a complete fracture**, with one half of the fractured specimen falling into the molten steel.

Chemical compositions of the steel specimens

	C (wt%)	Al (wt%)	Si (wt%)	T.O (ppm)
Steel reference	0.063	0.46	0.017	56.3
with AM	**0.071**	**0.24**	**0.078**	**11.7**
with A	0.47	0.29	0.16	52.2

Filter AM reduced the T.O content from **56.3 ppm to 11.7 ppm**.

Filter A did not significantly reduce the T.O content, which was possibly related to its fracture and subsequent fall into the molten steel.

Results and discussion

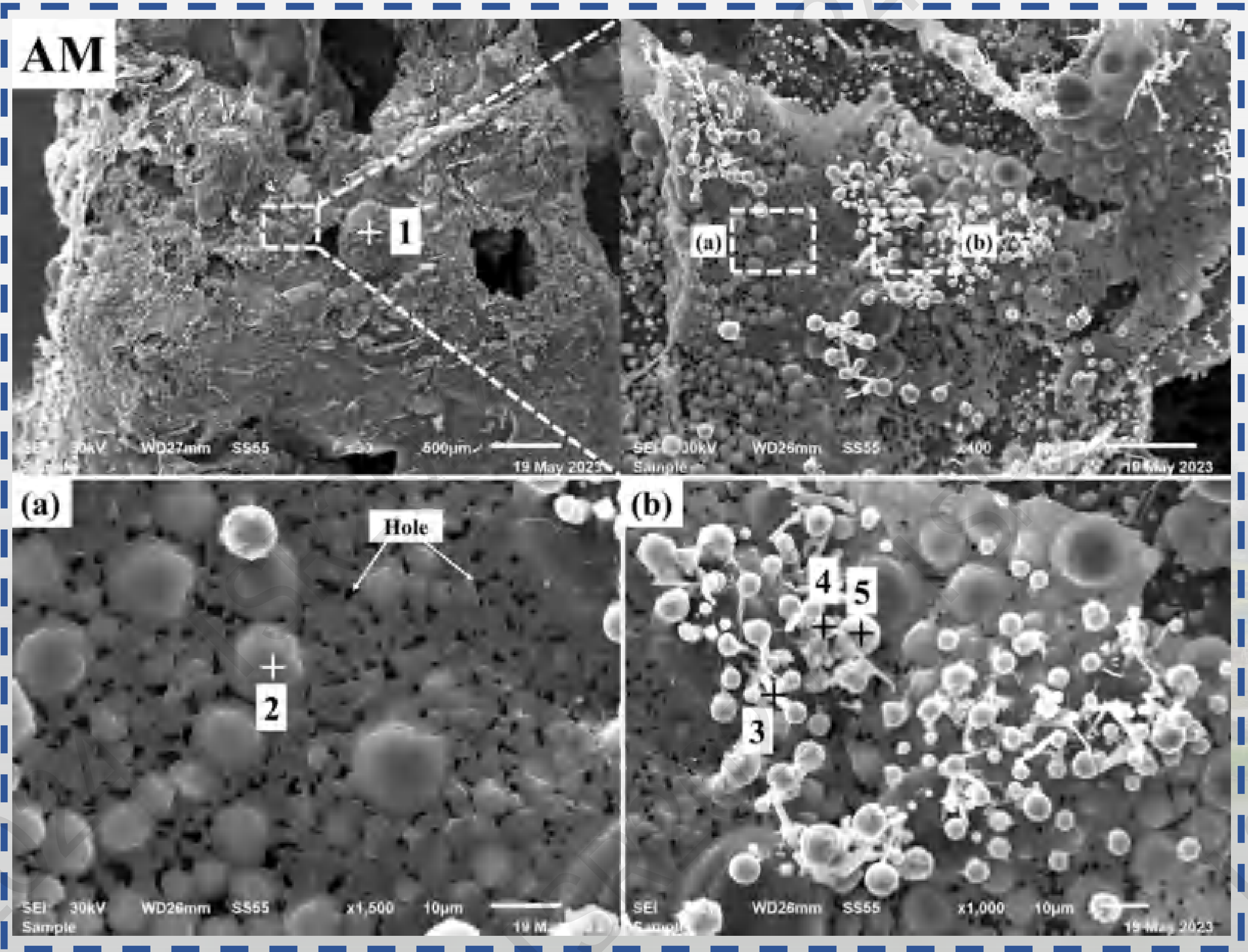

EDS results (At%)

	O	Mg	Al	Si	Cr	Fe	Possible phases (1600℃)
1	29.81	12.73	55.85			1.61	Corundum, Spinel
2	34.39	10.78	53.76			1.07	Corundum, Spinel
3	18.82	8.83	32.26	13.80	0.98	25.31	Olivine, Corundum, Composite Spinel
4	43.04	9.28	41.74	5.94			Corundum, Spinel, Olivine
5	4.65	7.45	17.79	17.89	1.89	50.33	Fe-Si-Al Alloy, Composite Spinel

Al_2O_3-$MgAl_2O_4$ reaction layer was observed on the surface of the filter, **exhibiting a significant distribution of micropores across its irregular surface.** It is observed **that Al_2O_3-$MgAl_2O_4$ and Al_2O_3-MgO-SiO_2 inclusions** in the molten steel were adsorbed on the surface of the porous Al_2O_3-$MgAl_2O_4$ layer.

Results and discussion

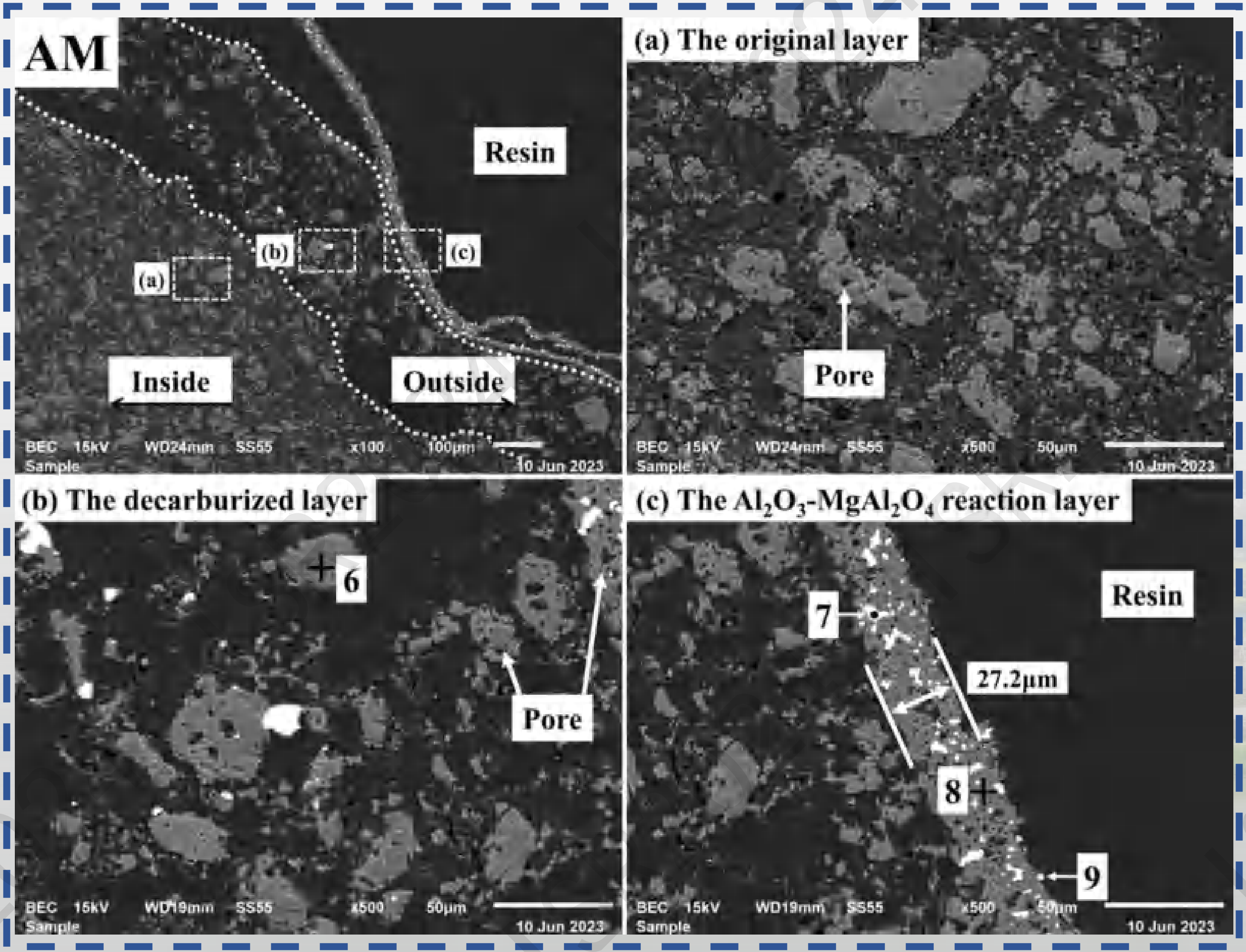

EDS results (At%)

	O	Mg	Al	Si	Fe	Possible phases (1600°C)
6	50.22	9.74	40.04			Corundum, Spinel
7			4.60		95.40	Fe-Al Alloy
8	42.59	18.68	38.15		0.58	Composite Spinel
9			2.55	18.92	78.53	Fe-Si-Al Alloy

(a) The original layer, located far from the molten steel, retained its original morphology;
(b) The decarburized layer, located near the molten steel, **experienced intense carbothermal reduction reactions**, resulting in a loose structure;
(c) The Al_2O_3-$MgAl_2O_4$ reaction layer, **in direct contact with the molten steel**, had a uniform thickness of approximately **27.2 μm**.

Results and discussion

武漢科技大学
WUHAN UNIVERSITY OF SCIENCE AND TECHNOLOGY

Discussion

Firstly, porous Al_2O_3-$MgAl_2O_4$ micropowder **facilitated the formation of β-SiC whiskers** within the filter.

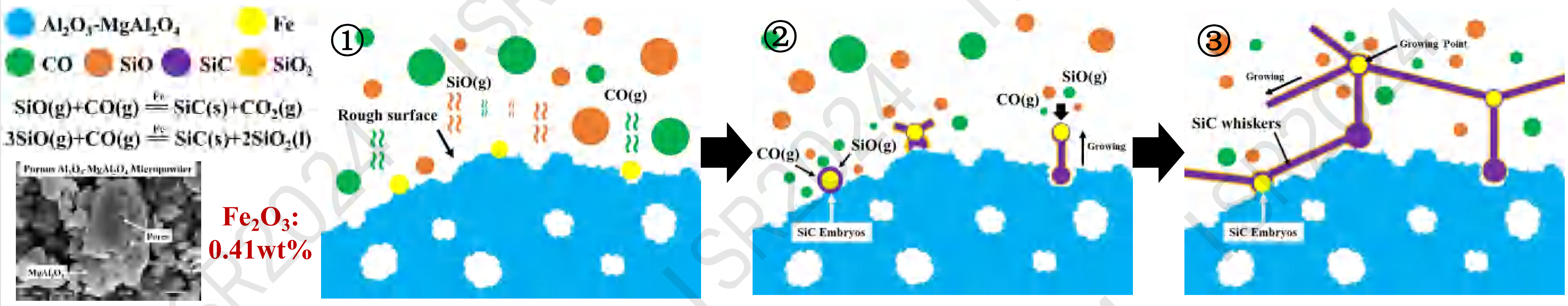

$$2C(s)+O_2(g)=2CO(g) \quad (1)$$

$$2Si(s)+O_2(g)=2SiO(g) \quad (2)$$

$$SiO(g)+3CO(g)=SiC(s)+2CO_2(g) \quad (3)$$

$$3SiO(g)+CO(g)=SiC(s)+2SiO_2(l) \quad (4)$$

The β-SiC whiskers branched out and epitaxially grew, originating from **the Fe catalyst droplets**, **forming a uniformly distributed β-SiC whisker network**.

Results and discussion

Discussion

Secondly, **the β-SiC** and **$MgAl_2O_4$ phase** significantly enhanced the thermal shock resistance of the filter.

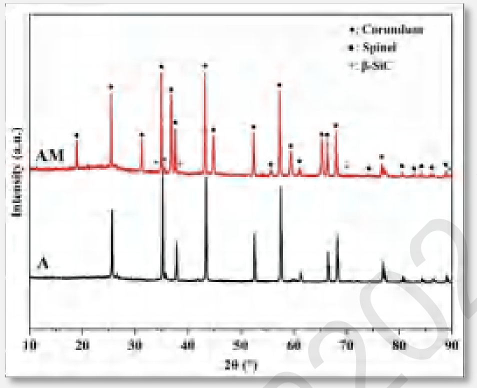

Porous Al_2O_3-$MgAl_2O_4$ micropowder (90.01 wt% Al_2O_3, 8.60 wt% MgO)

Relative contents of phase (XRD results)

Filter	Corundum	Spinel	β-SiC
AM	58 wt%	33 wt%	9 wt%
A	97 wt%	-	3 wt%

Spinel:

$MgAl_2O_4$

● : Mg

● : Al

○ : O

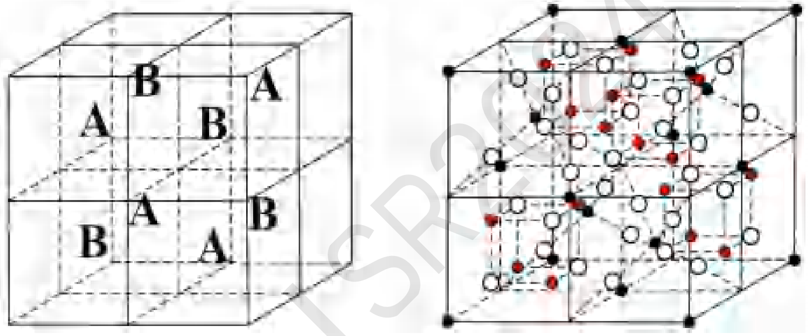

Filter AM exhibited a retention rate of 91.11% in its cold compressive strength after three thermal shock tests.

The **β-SiC whiskers interlocking porous Al_2O_3-$MgAl_2O_4$** and carbon particles in the filter AM **prevented the crack propagation** during the immersion test, so that no large cracks occurred in the filter AM.

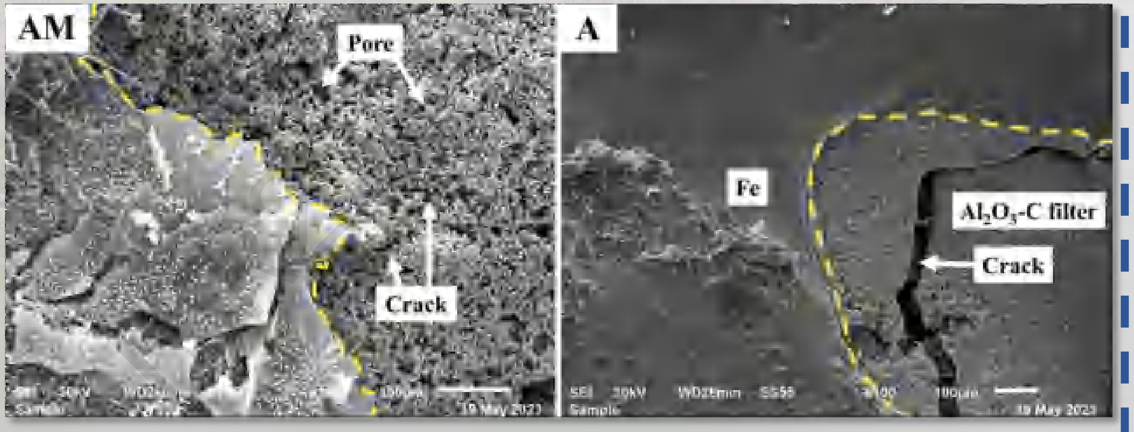

Results and discussion

WUHAN UNIVERSITY OF SCIENCE AND TECHNOLOGY

Discussion

Thirdly, the combination of the **microporous structure and $MgAl_2O_4$ phase** synergistically improved the **purification efficiency** of the filter for molten steel.

High purity argon
O_2 is less than 1ppm

$P(O_2) \leq 1*10^{-1}$ Pa

Based on the experimental conditions, the process of interfacial reactions between filter AM and the molten steel will be discussed from **the carbothermal reaction stage, the reaction layer formation stage and the final stage**.

Schematic illustration of immersion test using filter AM

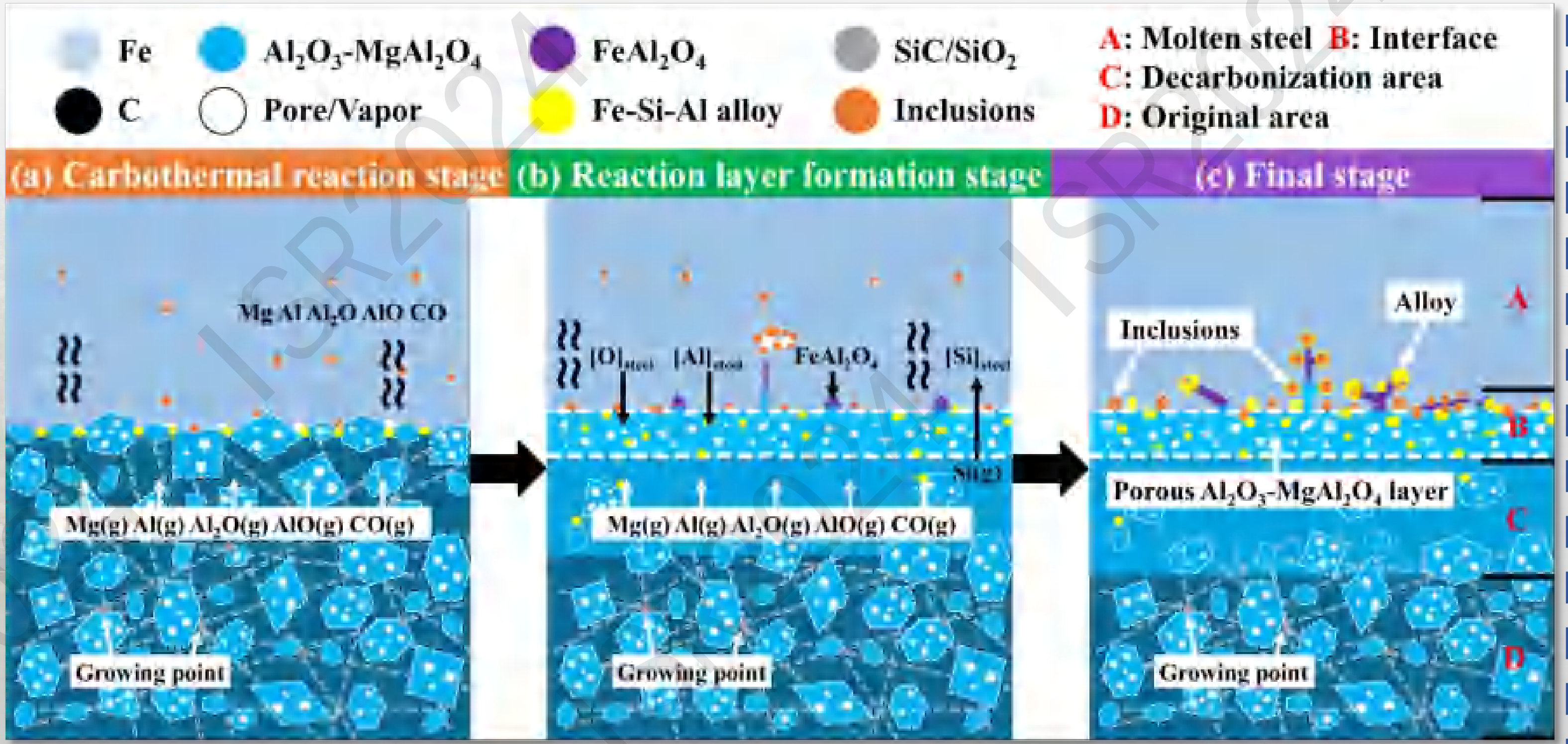

Results and discussion

Discussion (a) Carbothermal reaction stage

Carbothermal reaction stage

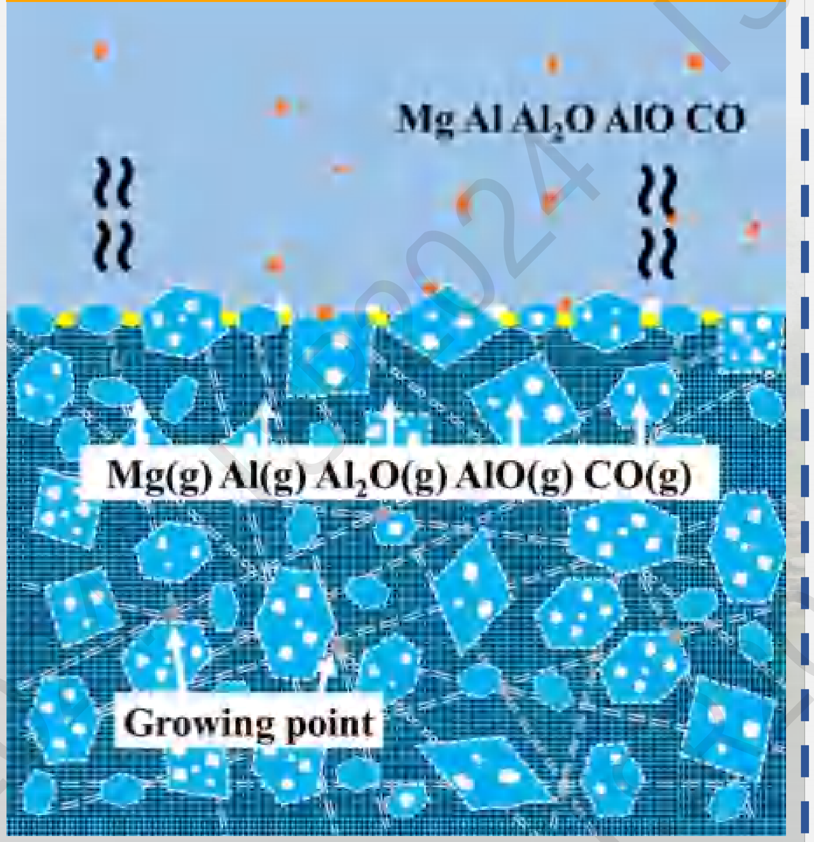

$Al_2O_3(s)+3C(s)=2Al(g)+3CO(g)$

$Al_2O_3(s)+2C(s)=Al_2O(g)+2CO(g)$

$Al_2O_3(s)+C(s)=2AlO(g)+CO(g)$

$2Al_2O_3(s)+9C(s)=Al_4C_3(s)+6CO(g)$

$MgAl_2O_4(s)+4C(s)=Mg(g)+2Al(g)+4CO(g)$

$MgAl_2O_4(s)+3C(s)=Mg(g)+Al_2O(g)+3CO(g)$

$MgAl_2O_4(s)+2C(s)=Mg(g)+2AlO(g)+2CO(g)$

$2MgAl_2O_4(s)+11C(s)=2Mg(g)+Al_4C_3(s)+8CO(g)$

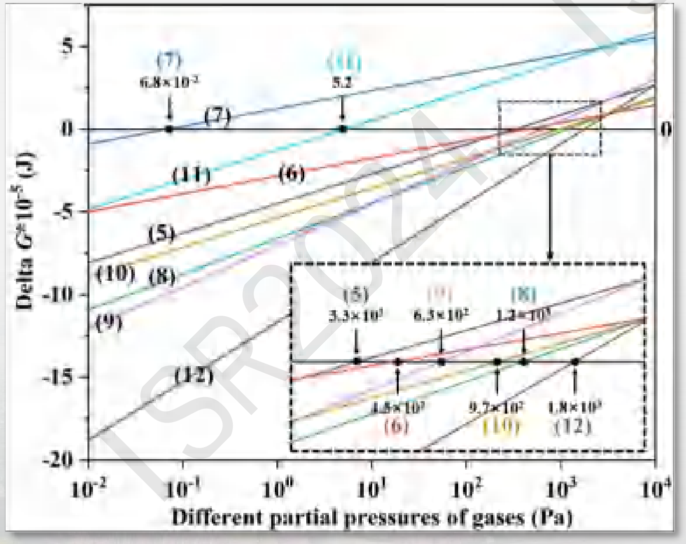

Al (g): 6.3×10^2 Pa

Al_2O (g): 9.7×10^2 Pa

AlO (g): 5.2 Pa

Mg (g): 1.8×10^3 Pa

CO (g): 1.8×10^3 Pa

Results and discussion

武漢科技大学
WUHAN UNIVERSITY OF SCIENCE AND TECHNOLOGY

Discussion

(b) Al_2O_3-$MgAl_2O_4$ reaction layer formation stage

Reaction layer formation stage

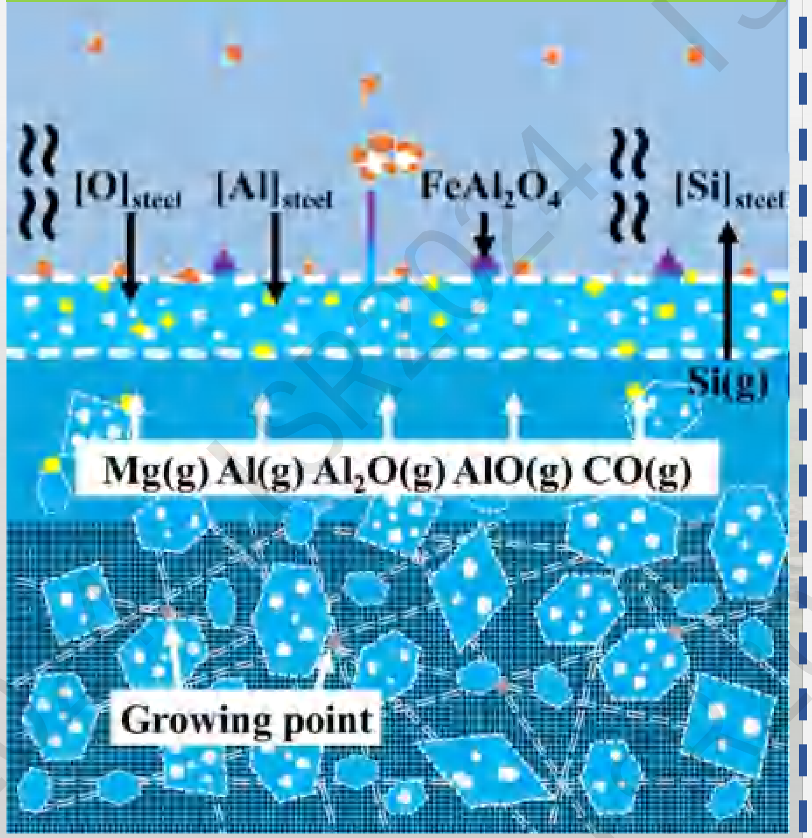

$Al_xO_y(g)+O_2(g)/[O]_{steel}=Al_2O_3(s)$

$Al_xO_y(g)+O_2(g)\ /[O]_{steel}+Fe(l)=FeAl_2O_4(s)$

$Al_xO_y(g)+O_2(g)/[O]_{steel}+Mg(g)=MgAl_2O_4(s)$

$2[Al]_{steel}+3[O]_{steel}=Al_2O_3(s)$

$Fe(l)+[O]_{steel}+Al_2O_3(s)=FeAl_2O_4(s)$

$2[Al]_{steel}+4[O]_{steel}+Mg(g)=MgAl_2O_4(s)$

$Si(g)=[Si]_{steel}$

Predominance area diagram of the Al-Mg-Fe-O-C system at 1600℃

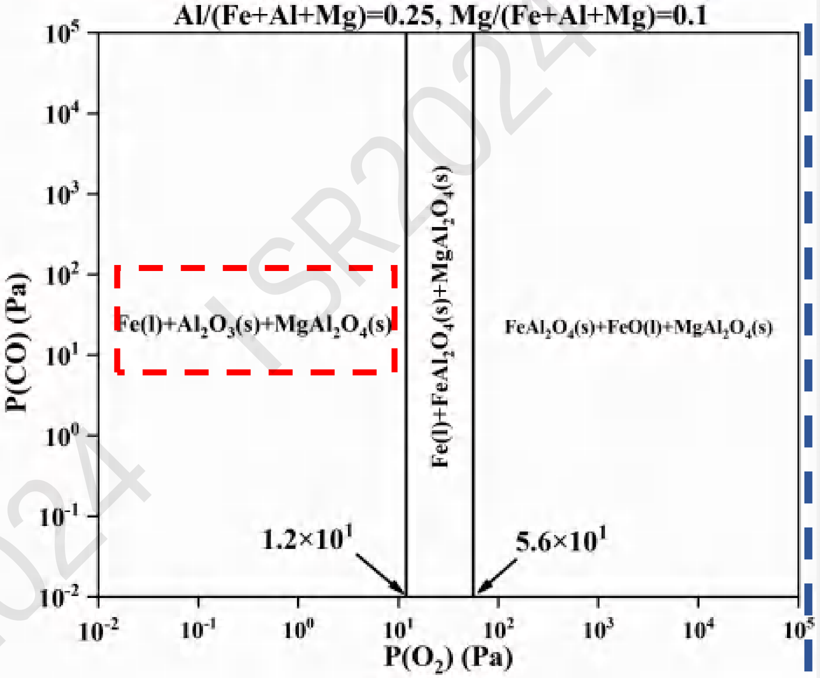

$FeAl_2O_4$ is the stable phase when the partial pressure of O_2 is **higher than 1.2×10¹ Pa** and **Al_2O_3 is the stable phase** when the partial pressure of O_2 is **lower than 1.2×10¹ Pa**.

厚德博學 崇實去浮

Discussion

(c) Final stage

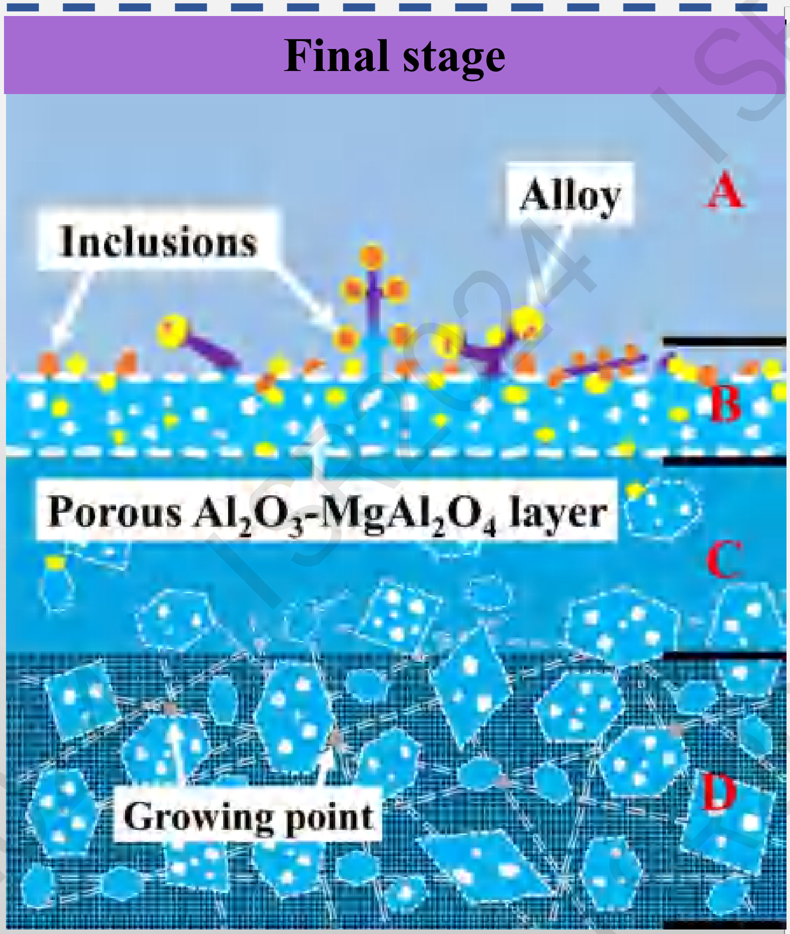

A: Molten steel

B: Interface

C: Decarbonization area

D: Original area

The filter AM had a rougher surface structure, where the aforementioned reaction process led to **the formation of the Al_2O_3-$MgAl_2O_4$ layer and $FeAl_2O_4$ nuclei.** As the inclusions were continuously and gradually adsorbed, **the Al_2O_3-$MgAl_2O_4$ layer progressively thickened, accompanied by the formation of acicular composite spinel on the surface.** The Fe on the surface dissolved the Al and Si vapors to form Fe-Si-Al alloy spheres, **which encapsulated the inclusions on the filter surface and linked with the porous layer through acicular composite spinel.**

4

—— PART FOUR ——

Conclusions

武汉科技大学
Wuhan University of Science and Technology

Conclusions

- The porous Al_2O_3-$MgAl_2O_4$ micropowder contained more **Fe_2O_3**. With the progress of VLS mechanism, β-SiC embryos formed on the rough grains surface under the catalysis of Fe, **leading to the development of a network structure of β-SiC whiskers**.
- The **β-SiC** and **$MgAl_2O_4$** phase significantly enhanced the **thermal shock resistance** of the filter. After three thermal shock tests, the cold compression strength of filter AM (0.41 MPa) was higher than that of filter A (0.36 MPa), with a strength retention rate as high as 91.11%.
- The combination of the **microporous structure and $MgAl_2O_4$** phase synergistically improved the **purification efficiency** of the filter for molten steel.

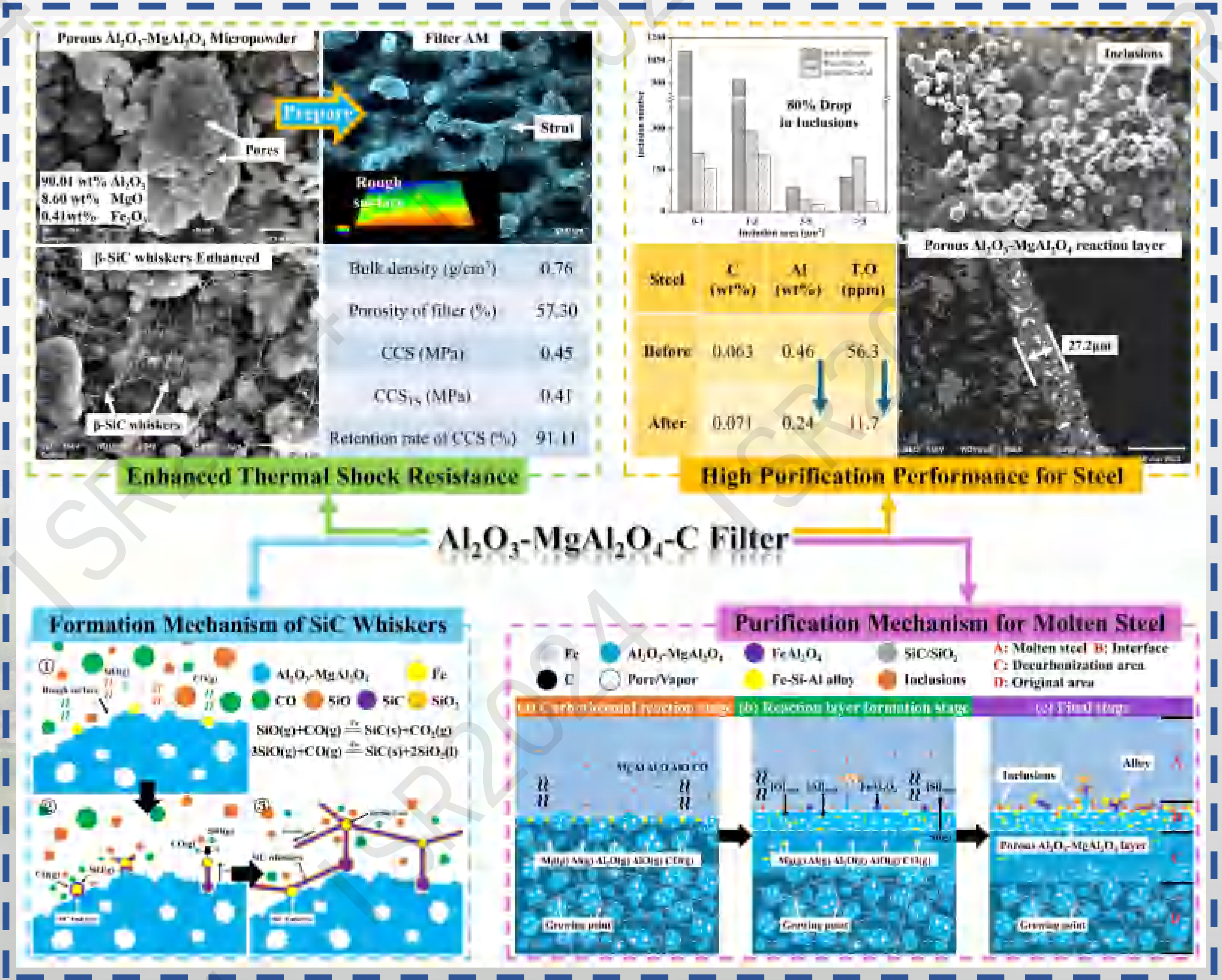

武漢科技大學
WUHAN UNIVERSITY OF SCIENCE AND TECHNOLOGY

Thank you for your listening!

PLEASE GIVE ME AS MUCH CRITICISM AS POSSIBLE

Jinwen Song | Supervisor: Prof. Wen YAN